

Eight-Port Tapered-Edged Antenna Array With Symmetrical Slots and Reduced Mutual-Coupling for Next-Generation Wireless and Internet of Things (IoT) Applications

Original Scientific Paper

Bilal A. Khawaja

Faculty of Engineering, Department of Electrical Engineering,
Islamic University of Madinah,
P. O. BOX 170 Madinah, 41411, Saudi Arabia
7166@iu.edu.sa, bam.khawaja@gmail.com

Abstract – A compact and low-cost eight-port (2x4 configuration) tapered-edged antenna array (TEAA) with symmetrical slots and reduced mutual-coupling is presented in this paper using the inset-feed technique. The 8-port TEAA is designed and simulated using CST microwave studio, fabricated using the flame-resistant (FR4) substrate having a dielectric constant (ϵ_r) = 4.3 and thickness (h) = 1.66mm and characterized using Keysight technologies vector network analyzer (VNA). The designed 8-port TEAA operates at the 5.05-5.2GHz frequency band. Various performance design parameters, like return-loss, bandwidth, gain, 2D/3D radiation patterns, surface current distributions, and isolation-loss, are briefly studied, and the results are summarized. The eight-port TEAA has featured the bandwidth/gain characteristic of 195MHz/10.25dB, 3dB beam-width of 52.8°, and excellent mutual-coupling (high isolation-loss) of less than -20dB, respectively. The 8-port TEAA is proposed and characterized to work for next-generation high-throughput WLANs like IEEE 802.11ax (WiFi-6E), Internet-of-Things (IoT), and the upcoming 5G wireless communication systems.

Keywords: Antenna array, IEEE 802.11ax, WiFi-6E, Internet-of-Things (IoT), 5G

1. INTRODUCTION

During the last 15 years, the world has seen a rapid upsurge in the use of wearable smart gadgets and hand-held wireless devices like smartwatches, smart glasses, fitness bands, etc., and mobile phones and tablets, respectively [1, 2]. The end-users are dependent on these devices for their day-to-day tasks, which vary from financial transactions to grocery shopping, online education to work-from-home business users, food delivery to live-streaming of videos and sports events, Metaverse-type online gaming as well as usage of artificial intelligence (AI) chatbots and social media applications, and smart-home monitoring to smart-farming solutions are to name the few [1-5]. This dependency is due to the advancement in the currently deployed 5G and future high-throughput wireless systems [1-3], [6]. The wireless end-users are exponentially growing, and it is estimated that by 2025, there will be 75 billion wireless devices linked to the Internet, up from the current figure of ~23 billion [7]. In order to uphold this ever-increasing demand for commercial and residential wireless end-users, IEEE has standardized an upgraded version of IEEE 802.11ac [8]

Wi-Fi, which is also known as IEEE 802.11ax (WiFi-6) [8]. In comparison to 802.11ac, the 802.11ax can achieve an overall 37% increase in the data-rates, which is equivalent to a data-transmission speed of 9.6GB/s [8]. Another enhancement of WiFi-6 is the 2.4GHz and 5GHz dual frequency band operation as compared to the single-band operation of IEEE 802.11ac, which only operates at 5GHz. In the years to come, enhanced wireless systems standards like WiFi-6E [8] will also be available, which are also referred to as high-throughput wireless local area networks (WLANs) [1, 2, 6, 8]. WiFi-6E systems will operate in the triple frequency bands of 2.4GHz/5GHz and 6GHz, respectively [8].

The main reason for the technological advancement of currently available WLAN standards and the enhancement of the next-generation of high-throughput WLANs like WiFi-6E, as well as the 5G wireless systems, is the requirement for antennas that are compact, exhibit wide bandwidth, and can be easily integrated with the upcoming wireless devices and systems. In modern WLAN systems, planar antennas are typically used, which are referred to as microstrip patch an-

tennas (MPAs) [9]. The reasons MPA based on planar structures are preferred in modern wireless systems, because of low-cost, low-profile, ease-of-design, compatibility, and conformality with the printed circuit boards (PCBs) [8-10]. A conventional MPA resonates at a single frequency and offers reduced gain and narrow bandwidth. Although by the insertion of different stubs and slots to change the current path on the resonating patch, the MPA can be made to oscillate at multiple frequency bands [8-10]. Using the MPA design techniques, many researchers [10-15] have proposed different antenna array designs for the 5G wireless systems operating at both microwave and mmW frequency bands [12].

Recently, there has been much interest in the multi-port antenna array systems which can operate and cover the frequency bands of next-generation high-throughput WLANs like WiFi-6/WiFi-6E, and the upcoming 5G system [16-21]. Multi-port antenna structures are preferred and selected by a number of researchers because they offer the benefit of physical antenna size reduction and also reduce the need for antenna-feeding networks, also referred to as beam-forming networks for phased array antenna systems [22]. In [16], an eight-element single-polarization linear array antenna has been proposed to enhance the isolation by using the decoupling ground (DG) technique. The array was operating at the 4.8-5GHz band and exhibited a gain of 7.3dB. Then, authors in [17] presented a 3.3-5GHz band operation wideband eight-port antenna array for 5G new radio (5G-NR) applications by employing defected ground structure (DGS) to achieve high isolation between radiating elements. Also, researchers in [18] presented an eight-port antenna system design for future 5G mobile broadband services operating in the C-band at the 5GHz band and demonstrated a gain of 7.4dB, respectively. In [19], an 8-element array is proposed for 5G systems operating at 3.27-5.92GHz based on L-shaped open slot antennas with an increased size of $150 \times 75 \text{ mm}^2$. An 8-element antenna array is proposed for 5G-NR and WiFi-6 applications by using the gap-coupled feeding technique and open-stub for improved bandwidth. The array achieved a gain of 4dB, which is considered relatively quite low for multi-port antenna systems [20]. Lastly, in [21], the authors presented an 8-element antenna array operating at 5.15-5.97GHz frequency band for 5G systems. The proposed antenna system uses a hybrid combination of modified Minkowski and Peano curves [14] fractal geometries. The proposed array [21] achieves good isolation of over 10dB between the antenna elements, although exhibited a reduced gain of 4dB only. The research study [16-21] shows that most of the researchers were trying to improve the bandwidth and mutual-coupling between the element of 8-port antenna arrays by using different complex techniques like DG and DGS. This leads to improved bandwidth and mutual-coupling but also results in reduced antenna array gain and larger-sized structures. Although, in this paper, the proposed 8-port

array exhibits an overall size reduction of 55% with a much-improved gain as compared to other similar designs. Moreover, it also shows an excellent mutual-coupling without using complicated design techniques.

So, in this work, the authors initially present a single-element antenna with tapered edges and symmetrical slots in the oscillating patch with an inset-feed technique using the FR4 substrate for low-cost implementation of the design. All the required antenna performance parameters are then briefly studied, and the results are compared. Then, an 8-port (2x4 configuration) tapered-edged antenna array (TEAA) has been proposed and studied using the single-element antenna design. The 8-port TEAA is proposed and designed to work for the next-generation of high-throughput WLANs like WiFi-6E, sub-6GHz 5G systems, and Internet of Things (IoT) and C-band applications [3, 5, 8]. The proposed single-element antenna and 8-port TEAA are designed to operate in the 5GHz frequency band. The proposed 8-port TEAA in this work has many attractive features, such as a high-gain and maximum intensity of radiation pattern at 45° . These features make the 8-port TEAA a worthy candidate for the upcoming high-throughput WLANs, sub-6GHz 5G, IoT, and next-generation wireless applications. All the 8-elements of the 2x4 configuration TEAA are individually fed using SMA connectors. Another salient feature of the proposed 8-port TEAA is that it exhibits reduced mutual-coupling (i.e., high isolation-loss) between the antenna elements, which is one of the critical requirements for the antenna arrays designed to work for next-generation WLAN applications.

The structure of the paper is as follows: Single-element antenna design parameters, simulation, and measurement results like return-loss (S_{11}), 2D/3D radiation patterns, and surface current distribution are studied and summarized in Section 2. In Section 3, the 8-port (2x4 configuration) tapered-edged antenna array, design, and characterization results are discussed. In addition to all of the above performance parameters, the isolation-loss is also studied for the 8-port array to study the mutual-coupling effects between the antenna elements of the array. Section 4 provides a comparison of the results with other researchers' work, and finally, Section 5 concludes the paper.

2. SINGLE-ELEMENT ANTENNA DESIGN AND CHARACTERISATION RESULTS

Initially, a single-element antenna is proposed and designed with tapered edges and symmetrical slots in the oscillating patch, as shown in Fig. 1(a-c). The inset-feed technique is also employed in this design to achieve better impedance matching between the 50 Ω feed-line and the oscillating patch. The substrate used to design and realize the antenna is FR4 having the thickness (h), dielectric constant (ϵ_r), and loss-tangent ($\tan \delta$) of 1.6mm, 4.3, and 0.025, respectively.

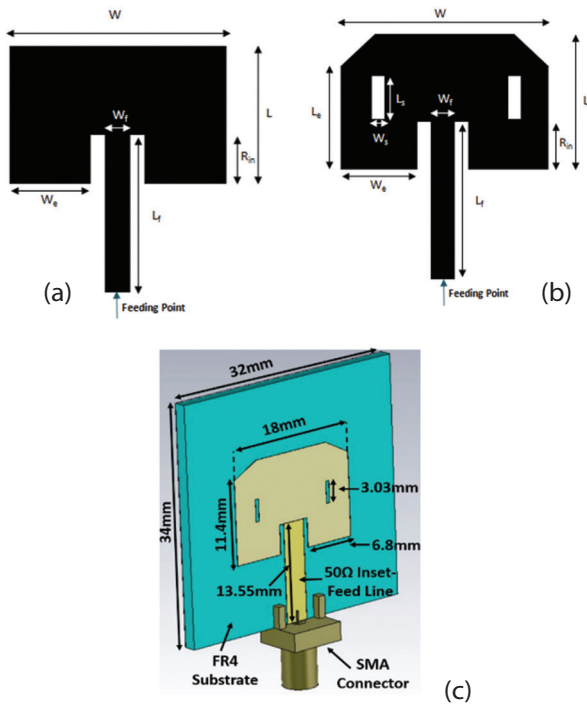


Fig. 1. (a) Basic rectangular MPA with inset-feed (b) Modified and optimized tapered-edged MPA with symmetrical slots (c) Layout of the final single-element antenna design from CST-MWS with dimensions

The patch antenna's initial calculations were conducted using the transmission-line model [9-10]. All the respective formulas are given below in Eq. (1) – (5):

$$L = L_{eff} - 2\Delta L \quad (1)$$

$$L_{eff} = \frac{c}{2f\sqrt{\epsilon_{reff}}} \quad (2)$$

$$\epsilon_{reff} = \frac{\epsilon_r + 1}{2} + \frac{\epsilon_r - 1}{2} \left[\frac{1}{\sqrt{1 + 12 \frac{h}{W}}} \right] \quad (3)$$

$$\Delta L = 0.412h \frac{[\epsilon_{reff} + 0.3] \left[\frac{W}{h} + 0.264 \right]}{[\epsilon_{reff} - 0.258] \left[\frac{W}{h} + 0.8 \right]} \quad (4)$$

$$W = \frac{c}{2f} \sqrt{\frac{2}{\epsilon_r + 1}} \quad (5)$$

Where:

L = Actual length of the patch

W = Actual width of the patch

L_{eff} = Effective length of the patch

ϵ_{reff} = Effective dielectric constant of the patch

ΔL = Extended incremental length of the patch

CST Microwave Studio (CST-MWS) has been used to design, analyze and simulate the different antenna parameters. The overall size of the proposed antenna is 34 mm × 32 mm, as shown in Fig. 1(c).

The resonating patch of the antenna was designed to resonate at 5.2GHz. Fig. 1(c) and Table 1 shows the proposed antenna dimensions.

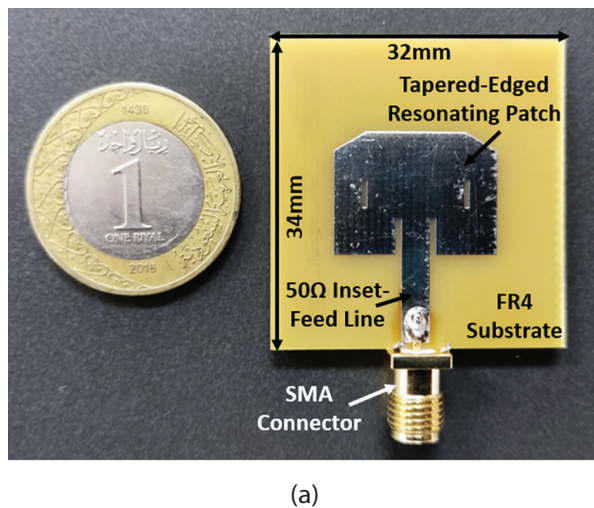
Table 1. Proposed single-element antenna dimensions.

Parameter	Dimensions (mm)
W	18
L	13.4
L_f	13.55
W_f	3.1
L_s	3.03
W_s	0.5
L_e	11.4
W_e	6.8
R_{in}	4

The final design of the single-element antenna is shown in Fig. 1(c), which is used to fabricate the antenna prototype. The FR4 substrate-based fabricated prototype of the single-element tapered-edged antenna with symmetrical slots, inset-feed and complete ground-plane is shown in Fig. 2(a). The single-element antenna was characterized using Keysight Technologies FieldFox N9916B Vector Network Analyzer (VNA), as shown in Fig. 2(b).

The antenna-under-test (AUT) connected to VNA Port-1 in Fig. 2(b) shows that the single-element antenna was resonating around the 5.2GHz frequency band. The comparison of the simulated and measured return-loss S_{11} [dB] curves of the proposed single-element tapered-edged antenna design is summarized in Fig. 3.

It can be seen from the simulated and measured S_{11} [dB] result that the simulated antenna was designed to resonate at the center frequency of 5.2GHz. Although the measured antenna response depicts a slight shift in the single-element antenna resonant center frequency which is now at 5.1GHz. This could be due to the fabrication tolerances, SMA connector soldering, and loss-tangent variation of the FR4 substrate.



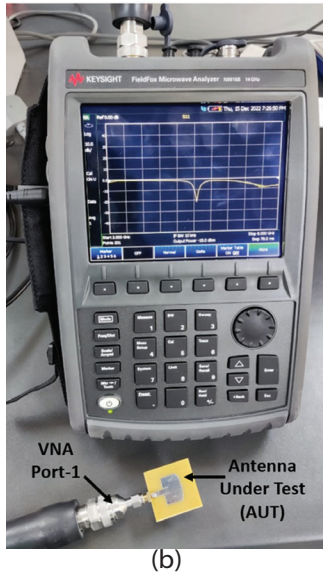


Fig. 2. (a) Fabricated prototype of single-element antenna using FR4 substrate, and (b) S-parameter measurement setup showing the single-element antenna connected to Keysight VNA for S_{11} [dB] measurement

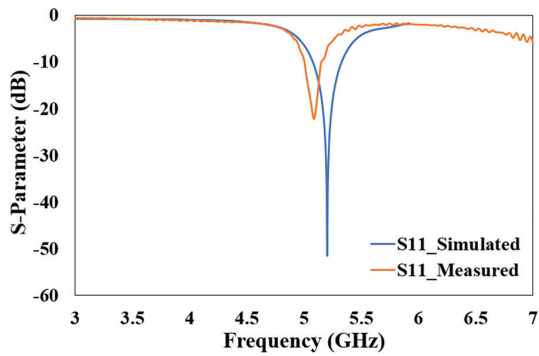


Fig. 3. Simulated and Measured S_{11} [dB] of the proposed single-element tapered-edged antenna with symmetrical slots, and inset-feed

It can also be observed from Fig. 3 that the simulated and measured S_{11} [dB] responses of the single-element antenna give the -10 dB resonant bandwidth of 248 MHz and 195 MHz, respectively. The S_{11} values also suggest good impedance matching at 50 Ω , and reasonable bandwidth. Based on the simulated and measured results, it was found that the impedance bandwidths range from 5.15-5.4 GHz and 5.05-5.2 GHz, with a voltage standing wave ratio (VSWR) that is less than 2 [9, 10]. The VSWR value of the proposed antenna indicates a stable and reliable performance.

Fig. 4 (a-c) now shows the simulated/measured 2D (E-plane/H-plane) and 3D radiation patterns (RPs) of the proposed single-element antenna, respectively. It can be seen from the E-plane and H-plane 2D RP in Fig. 4 (a-b) that the simulated and measured gain is 6.74 dB and 5 dB at 5.2 GHz, respectively. The 3D RP of the proposed single-element antenna is shown in Fig. 4(c). The antenna gain of 6.74 dB can be observed from Fig. 4(c)

at the resonant frequency of 5.2 GHz. The 2D simulated and measured RP results show that the antenna radiates maximum at 0° and 10° with fewer side lobes. It is more clear in the 3D RP that the antenna radiation in the boresight with respect to the structure.

After measuring the 2D and 3D RPs, the surface current distribution of the single-element antenna is also studied, and the results are compiled in Fig. 5. The surface current distribution graph of the resonating patch antenna shows that the current density is highest close to the tapered edges and around the symmetrical slots.

3. 8-PORT TAPERED-EDGED ANTENNA ARRAY (TEAA) DESIGN AND CHARACTERISATION RESULTS

Multiple-element antenna arrays, which offer high directionality, gain, and resonant bandwidth, are one of the critical requirements for the WiFi-6E WLANs, currently deployed 5G wireless systems, and next-generation of high-throughput wireless technologies [3, 6, 8, 10, 11, 16-21]. To design the N-elements antenna array, the mathematical Eq. (6) – (8) are used. The 8-port TEAA's total field is equal to the single-element at the origin multiplied by a factor usually referred to as the array factor (AF) [9,10].

$$E_{(Total)} = [E_{(Single\ Element\ at\ Reference\ Point)}] \times [AF] \quad (6)$$

For any N-element array with uniform amplitude and spacing, the AF is given by:

$$\Psi = (kd \cos\theta + \beta) \quad (7)$$

$$AF = \left[\frac{\sin\left(\frac{N}{2}\Psi\right)}{\sin\left(\frac{1}{2}\Psi\right)} \right] \quad (8)$$

Where:

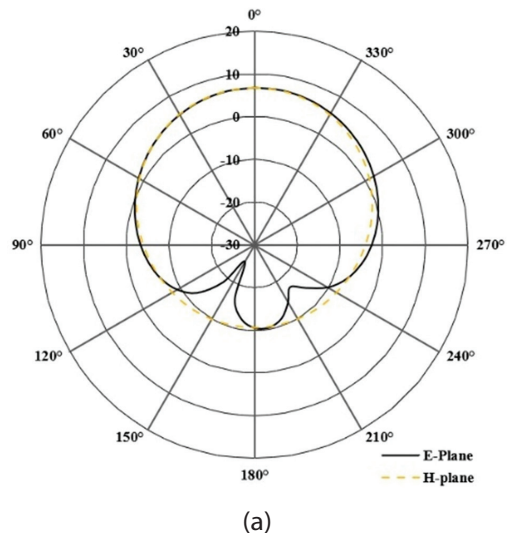
k = Wave number given by $2\pi/\lambda$,

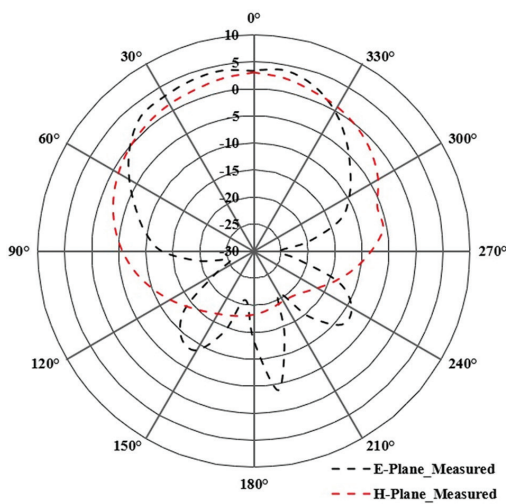
d = Distance between the array elements,

θ = Angle of the main beam of the antenna array,

β = Phase difference between individual elements,

N = No. of antenna elements in an array





(b)

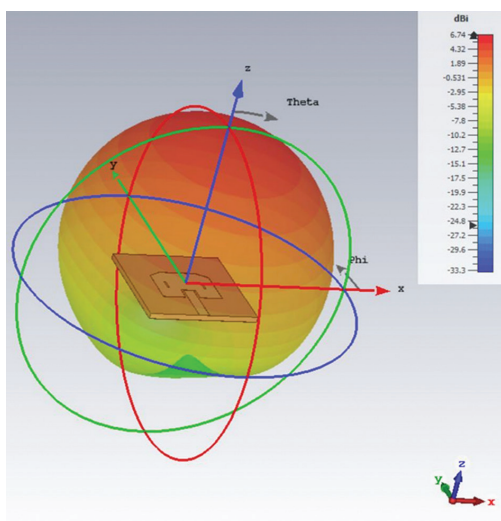


Fig. 4. (a) Simulated (b) Measured 2D (E-plane and H-plane) and (c) 3D Radiation Patterns of the proposed single-element tapered-edged antenna

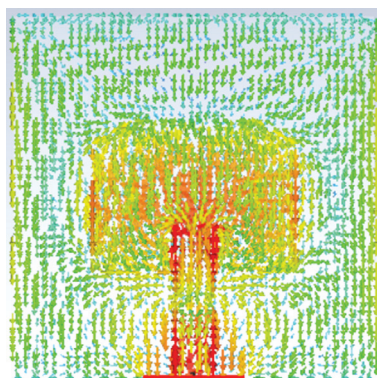
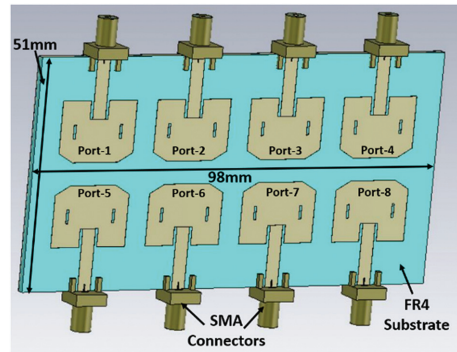


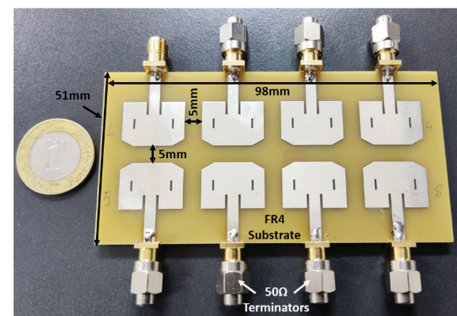
Fig. 5. Surface current distribution of the proposed single-element antenna

So, a 2x4 configuration (8-port) antenna array has been designed, fabricated, and characterized using the previously proposed single-element tapered-edged antenna, as shown in Fig. 6(a-c). The 8-port tapered-edged antenna array (TEAA) is also simulated using the CST-MWS to study its behavior, and fabricated/proto-

typed using FR4 substrate. The comparison of simulated and measured return-loss responses of the 8-port TEAA are summarized in Fig. 7(a-b).



(a)



(b)



(c)

Fig. 6. (a) Simulated design of the 8-Port TEAA using CST-MWS showing all the ports and SMA connectors (b) Fabricated FR4 prototype of 8-Port TEAA with dimensions (c) Keysight VNA-based S-parameter measurement setup of 8-port TEAA, where VNA Port-1 is connected to one port of TEAA and all other ports are terminated using 50Ω terminators

An important performance parameter in the antenna array design is the spacing between the array elements, which is kept at 5mm [9-12]. Moreover, the center-to-center inter-element spacing is a key factor for the reduction of radiation side-lobes and grating. Therefore, in the case of the 8-port TEAA, the center-to-center inter-element spacing is kept at $0.4 \lambda_0$, i.e., 23 mm. It can be observed from the return-loss results in Fig. 7(a-b) that the 8-port TEAA is operating in the 5.2 GHz band as desired. This makes the 8-port TEAA a worthy candidate for the currently deployed 5G wireless and IoT systems as well as for next-generation high-throughput WLAN operations. The 8-port TEAA proposed and realized in this work offers very good simulated/measured bandwidth characteristics of 248 MHz/195 MHz and simulated/measured return-loss responses in the range of -35 dB to -45 dB/-20 dB to -28 dB, at 5.2/5.1 GHz respectively.

After the return-loss results, the isolation-loss study is performed to understand the mutual-coupling behavior between the different antenna elements of the 8-port TEAA. Both simulated and measured results are compared and summarized, as shown in Fig. 7 (a-b). It can be seen from the results in Fig. 7 (a-b) that only the isolation-loss between the TEAA port-1 (antenna element-1) is measured with the rest of the antenna elements. Fig. 7 (a-b) shows very good inter-element isolation characteristics of the 8-port TEAA, and the simulated/measured isolation-loss in the range of -15 dB to -36 dB/-20 dB to -40 dB is achieved around the 5.2 GHz frequency band, respectively.

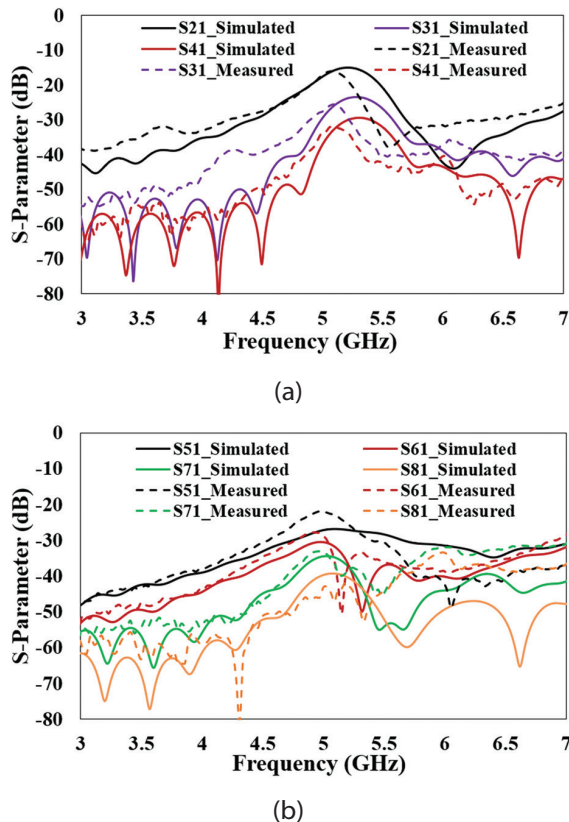


Fig. 7. Shows the simulated and measured isolation-loss of the 8-port TEAA (a) S_{21} - S_{41} [dB] (b) S_{51} - S_{81} [dB]

The isolation-loss study features the reduced mutual-coupling between the different antenna elements of the 8-port TEAA. The reduced mutual-coupling also shows that the proposed 8-port TEAA can be used as a good option for the deployment of the next-generation high-throughput WLANs and IoT systems. After performing the isolation-loss study, the simulated and measured 2D (E-plane and H-plane) RPs, 3D RPs, and the surface current distribution results of the 8-port TEAA are investigated to understand the behavior of the proposed TEAA for the upcoming next-generation high-throughput WLANs and currently deployed 5G wireless systems. Fig. 8 (a-b) compares the simulated and measured 2D E- and H-plane RPs of the 8-port TEAA at 5.2GHz, which shows that the gain is ~ 10.3 dB and ~ 10 dB, respectively, and the array antenna radiates maximum at 45° .

After the 2D RP, the 3D RP of the 8-port TEAA is studied at the oscillating frequency of 5.2GHz, and the results are summarized in Fig. 8 (c). It can be observed from the 3D RP in Fig. 8 (c) that at 5.2GHz resonance frequency, the TEAA exhibits a gain of 10.25dB, which demonstrates the directionality of the radiating electromagnetic waves from the proposed design. This is an important requirement for both high-efficiency next-generation WLANs and the currently deployed 5G wireless systems because it makes the smart-antenna beam-forming and beam-steering easier to implement [1-3,6, 9, 11, 12].

Fig. 9 shows the surface current distribution of the 8-port TEAA. It can be observed from the surface current distribution graph that it is high across the feeding line, edges of patches, and around the slots on the resonating patch antenna.

4. COMPARISON STUDY

This section will present a comparison of the 8-port TEAA presented in this paper with the similar 8-port antenna arrays proposed by other researchers in the literature [16-21]. The results are summarized in Table 2, which shows a comparison of the parameters like frequency of operation, No. of antenna elements in the array, antenna array size, gain, and mutual-coupling characteristics.

Table 2. A comparison study of the 8-port TEAA with existing designs

Ref.	No. of Array Elements	Frequency Band (GHz)	Size (mm ²)	Gain (dB)	Mutual-Coupling (dB)
[16]	8	4.8-5	300 × 60	7.3	<-27
[17]	8	3.3-5.45	150 × 75	3.5	<-18
[18]	8	4.8-5	150 × 75	7.4	<-10
[19]	8	3.27-5.92	150 × 75	-	<-10
[20]	8	5.18-7.71	-	4	<-18
[21]	8	5.15-5.97	150 × 75	4	<-10
[This Work]	8	5.15-5.4	98 × 51	10.25	<-20

The comparison study presented in Table 2 shows that the previous designs [16-21] presented in the table are more focused on improving mutual-coupling by using different techniques, while also attempting to enhance the bandwidth without much improvement in gain. The results of the proposed 8-port TEAA design show that the size of the array antenna is reduced by 55%, while the gain is drastically improved.

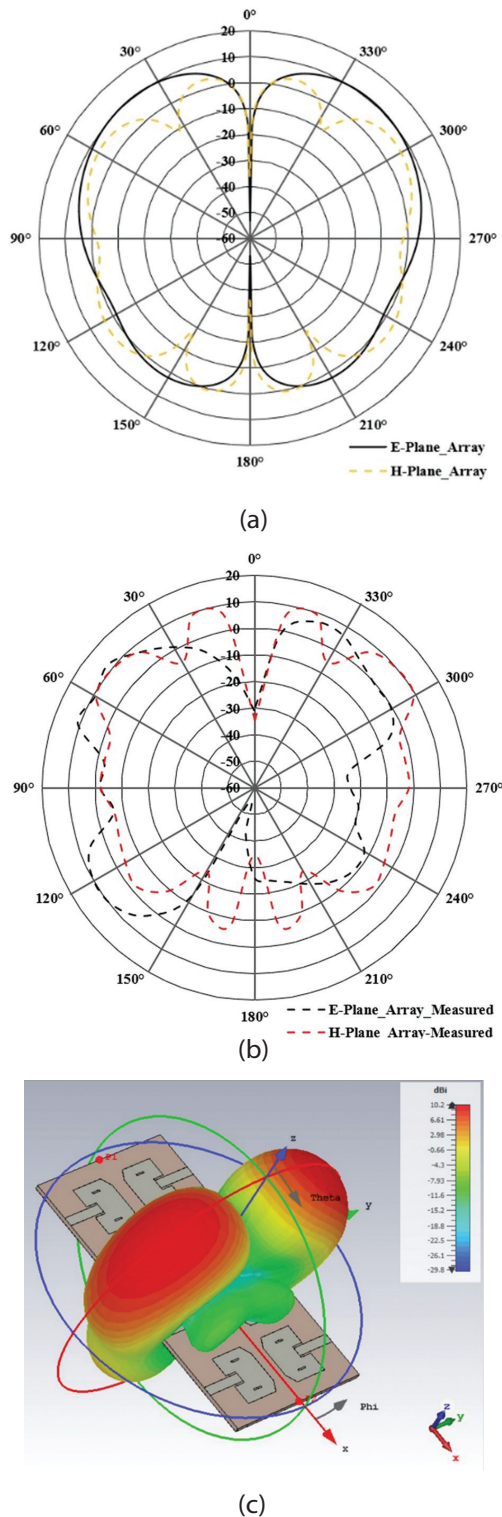


Fig. 8. (a) Simulated (b) Measured 2D (E-plane and H-plane) and (c) 3D Radiation Patterns of the proposed 8-port TEAA at 5.2GHz

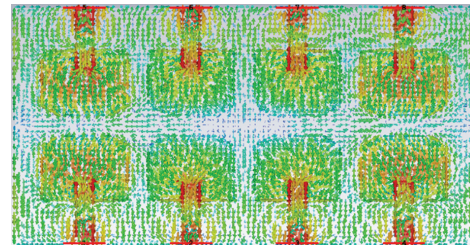


Fig. 9. Surface current distribution of the proposed 8-port TEAA at 5.2GHz

Moreover, the results demonstrate excellent reduced mutual coupling characteristics as compared to previous designs without using complicated design techniques.

5. CONCLUSION

This paper initially presented a single-element antenna with tapered edges and symmetrical slots in the oscillating patch by employing the inset-feed technique for 5.2 GHz frequency band operation. The proposed antenna has shown the bandwidth/gain characteristic of 195 MHz/6.74 dB, and the 3 dB beam-width is 84.5°. Then, by employing the single-element antenna design structure, an eight-port (2x4 configuration) tapered-edged antenna array (TEAA) has been proposed. Both single-element antenna and eight-port TEAA are realized using FR4 substrate for low-cost implementation of the design. The proposed eight-port TEAA covers the 5.05-5.2 GHz frequency band. The eight-port TEAA has also featured the bandwidth/gain characteristic of 195MHz/10.25 dB, 3 dB beam-width of 52.8°, and excellent mutual-coupling (high-isolation loss) of less than -20 dB. All of these features and the reduced-sized structure of the eight-port TEAA make it an ideal candidate for next-generation high-throughput WLANs like WiFi-6E, Internet-of-Things (IoT), and the upcoming 5G wireless communication systems.

6. REFERENCES

- [1] O. Kanhere, H. Poddar, Y. Xing, D. Shakya, S. Ju, T. S. Rappaport, "A Power Efficiency Metric for Comparing Energy Consumption in Future Wireless Networks in the Millimeter-Wave and Terahertz Bands", *IEEE Wireless Communications*, Vol. 29, No. 6, 2022, pp. 56-63.
- [2] I. F. Akyildiz, C. Han, Z. Hu, S. Nie, J. M. Jornet, "Terahertz Band Communication: An Old Problem Revisited and Research Directions for the Next Decade", *IEEE Transactions on Communications*, Vol. 70, No. 6, Jun. 2022, pp. 4250-4285.
- [3] K. Shafique, B. A. Khawaja, F. Sabir, S. Qazi, M. Mustafaqim, "Internet of Things (IoT) for Next-Generation Smart Systems: A Review of Current Challenges, Future Trends and Prospects for Emerging 5G-IoT Scenarios", *IEEE Access*, Vol. 8, 2020, pp. 23022-23040.

- [4] S.-M. Park, Y.-G. Kim, "A Metaverse: Taxonomy, Components, Applications, and Open Challenges", *IEEE Access*, Vol. 10, 2022, pp. 4209-4251.
- [5] S. Qazi, B. A. Khawaja, Q. U. Farooq, "IoT-Equipped and AI-Enabled Next Generation Smart Agriculture: A Critical Review, Current Challenges and Future Trends", *IEEE Access*, Vol. 10, 2022, pp. 21219-21235.
- [6] T. S. Rappaport, Y. Xing, O. Kanhere, S. Ju, A. Madanayake, S. Mandal, A. Alkhateeb, G. C. Trichopoulos, "Wireless Communications and Applications Above 100 GHz: Opportunities and Challenges for 6G and Beyond", *IEEE Access*, Vol. 7, 2019, pp. 78729-78757.
- [7] Statista Research Department, "Internet of Things (IoT) connected devices installed base worldwide from 2015 to 2025", www.statista.com/statistics/471264/iot-number-of-connected-devices-worldwide/ (accessed: 2023)
- [8] E. Khorov, A. Kiryanov, A. Lyakhov, G. Bianchi, "A Tutorial on IEEE 802.11ax High Efficiency WLANs", *IEEE Communications Surveys & Tutorials*, Vol. 21, No. 1, 2019, pp. 197-216.
- [9] C. A. Balanis, "Antenna Theory, Analysis and Design", 3rd Edition, John Wiley & Sons, 2005.
- [10] H. Wong, K.-M. Luk, C. H. Chan, Q. Xue, K. K. So, H. W. Lai, "Small Antennas in Wireless Communications", *Proceedings of the IEEE*, Vol. 100, No. 7, 2012, pp. 2109-2121.
- [11] M. C. Tan, M. Li, Q. H. Abbasi, M. Imran, "A Wideband Beam forming Antenna Array for 802.11ac and 4.9 GHz", *Proceedings of the Antennas and Propagation 13th European Conference, Krakow, Poland, 31 March - 5 April 2019*, pp. 1-5
- [12] J. H. Kim, J. H. Han, J. S. Park, J. G. Kim, "Design of phased array antenna for 5G mm-wave beamforming system", *Proceedings of the IEEE 5th Asia-Pacific Conference on Antennas and Propagation, Kaohsiung, Taiwan, 26-29 Jul 2016*, pp. 201-202.
- [13] A. K. Vallappil, B. A. Khawaja, M. K. A. Rahim, M. N. Iqbal, H. T. Chattha, M. F. bin M. Ali, "A Compact Triple-Band UWB Inverted Triangular Antenna with Dual-Notch Band Characteristics Using SSRR Metamaterial Structure for Use in Next-Generation Wireless Systems", *Fractal and Fractional*, Vol. 6, No. 8, 2022, p. 422.
- [14] A. Karimbu Vallappil, M. K. A. Rahim, B. A. Khawaja, M. N. Iqbal, N. A. Murad, M. M. Gajibo, L. O. Nur, B. S. Nugroho, "Complementary split-ring resonator and strip-gap based metamaterial fractal antenna with miniature size and enhanced bandwidth for 5G applications", *Journal of Electromagnetic Waves and Applications*, Vol. 36, No. 6, 2022, pp. 787-803.
- [15] B. A. Khawaja, M. A. Tarar, T. Tauqeer, F. Amir, M. A. Mustaqim, "1 × 2 Triple Band Printed Antenna Array for Use In Next Generation Flying Ad-Hoc Networks (FANETs)", *Microwave and Optical Technology Letters*, Vol. 58, 2016, pp. 606-610.
- [16] S. Zhang, X. Chen, G. F. Pedersen, "Mutual Coupling Suppression With Decoupling Ground for Massive MIMO Antenna Arrays", *IEEE Transactions on Vehicular Technology*, Vol. 68, No. 8, Aug. 2019, pp. 7273-7282.
- [17] J. Cai, J. Zhang, S. Xi, J. Huang, G. Liu, "A Wideband Eight-Element Antenna with High Isolation for 5G New-Radio Applications", *Applied Sciences*, Vol. 13, No. 1, 2022, p. 137.
- [18] W. Wang, Y. Li, Y. Xu, W. Shen, "Compact 8-Port MIMO Antenna System for Dual-Band 5G Mobile Terminals", *Proceedings of the International Conference on Microwave and Millimeter Wave Technology, Chengdu, China, 2018*, pp. 1-3.
- [19] H.-D. Chen, Y.-C. Tsai, C.-Y.-D. Sim, C. Kuo, "Broadband Eight-Antenna Array Design for Sub-6 GHz 5G NR Bands Metal-Frame Smartphone Applications", *IEEE Antennas and Wireless Propagation Letters*, Vol. 19, No. 7, 2020, pp. 1078-1082.
- [20] K. R. Jha, N. Rana, S. K. Sharma, "Design of Compact Antenna Array for MIMO Implementation Using Characteristic Mode Analysis for 5G NR and Wi-Fi 6 Applications", *IEEE Open Journal of Antennas and Propagation*, Vol. 4, 2023, pp. 262-277.
- [21] Y. M. Muhsin, A. J. Salim, J. K. Ali, "An eight-element multi-band MIMO antenna system for 5G mobile terminals", *AIP Conference Proceedings*, Vol. 2651, 2023, p. 060005.
- [22] A. K. Vallappil, M. K. A. Rahim, B. A. Khawaja, N. A. Murad, M. G. Mustapha, "Butler Matrix Based Beamforming Networks for Phased Array Antenna Systems: A Comprehensive Review and Future Directions for 5G Applications", *IEEE Access*, Vol. 9, 2020, pp. 3970-3987.